ACS APPLIED POLYMER MATERIALS

pubs.acs.org/acsapm Article

Polyurea Networks from Moisture-Cure, Reaction-Setting, Aliphatic Polyisocyanates with Tunable Mechanical and Thermal Properties

Antoni Sánchez-Ferrer,* Viktor Soprunyuk, Max Engelhardt, Ralf Stehle, H. Albert Gilg, Wilfried Schranz, and Klaus Richter*

Cite This: *ACS Appl. Polym. Mater.* 2021, 3, 4070–4078 Read Online

ACCESS | Metrics & More | Article Recommendations | Supporting Information

ABSTRACT: A series of one-component aliphatic polyisocyanates has been synthesized and analyzed before and after the moisture-curing process. The resulting reactive polymers are monodisperse tetrafunctionalized reactive molecules that become aliphatic polyurea networks with enhanced tunability of mechanical, chemical, and thermal properties compared to polyurethane and polyamide counterparts. This tunability responds to the insertion of a soft polypropylene oxide polymer segment between two triisocyanate molecules, as demonstrated by two-dimensional diffusion ordered spectroscopy (2D DOSY) ^{1}H NMR experiments and confirmed by Fourier transform infrared (FT-IR) spectroscopy. After curing, the polyurea networks show two glass transition temperatures: a characteristic of microphase-segregated block copolymers and a transient network due to the presence of the hydrogen bonds between the urea motives, as concluded from the evaluation of dynamic mechanical analysis (DMA), wide-angle X-ray scattering (WAXS), small-angle X-ray scattering (SAXS), and differential scanning calorimetry (DSC) experiments. Therefore, controlling the volume fraction, i.e., the degree of polymerization of the polypropylene oxide soft domains, the cured materials exhibit viscoplastic or viscoelastic properties, making these polyurea networks very attractive as adhesives or sealants.

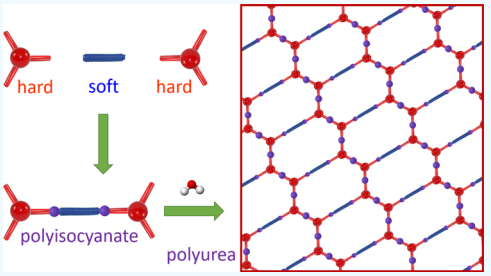

KEYWORDS: *reactive polymers, isocyanate, adhesives, moisture-cure, polyurea, network, viscoelastic, viscoplastic*

INTRODUCTION

Adhesives are used to bond a large range of materials, e.g., metals, glass, concrete, plastics, ceramics, and wood, with widespread uses in construction,[1] aerospace,[2] automotive,[3] packaging,[4] painting and coatings,[5] electrical engineering,[6] electronics,[7] microsystems technology,[8] footwear,[9] textile,[10] furniture,[11] foundry,[12] dentistry,[13] as well as in biomedical[14] and pharmaceutical[15] applications.

Reactive structural adhesives, which have to be wet and spread on the surface of the adherends, fill up the gap between the two surfaces and penetrate the structure of porous materials, as well as have the inherent property of transforming from a liquid to solid material by a chemical reaction.[16] During the curing reaction, the structural adhesive viscosity increases because of the formation of long amorphous polymer chains with a high glass transition temperature (thermoplastic adhesives) or small mesh size polymer networks (thermosetting adhesives) that bind to the surface of the adherends by a number of phenomena causing molecular adhesion, fill the voids between rough surfaces, and/or penetrate deep in the adherend's subsurface structure, producing mechanical interlocking.[17,18]

Reactive adhesives comprise reactive liquid monomers or oligomers, e.g., acrylic, methacrylic, cyanoacrylic, epoxide, or isocyanate adhesives, and solvent-based adhesives, e.g., aminoplastics or phenolics, using water or organic solvents for reducing the viscosity and reactivity.[19] While acrylic and methacrylic adhesives need an initiator and cannot establish covalent bonds with the adherend, the rest of the mentioned adhesives do so if nucleophilic groups, such as OH and NH_2, are present in the adherend.[20]

Isocyanate adhesives include a broad family of products that might be one-component or two-component adhesives, and they can be produced as solvent-free or solvent-based adhesives.[21] While the two-component adhesives are based on the formation of carbamates or urethane groups by reacting an isocyanate with a polyol, therefore, the polyurethane name applies, the one-component adhesives react with moisture and form urea linkages. Hence, the polyurea name describes the resulting chemistry better. From here onward, we will refer to the moisture-cure one-component isocyanate adhesives as polyurea. The complete curing time, which ranges from 12 to 72 h, strongly depends on the chemistry and structure of the reacting isocyanate, as well as the thickness of the adhesive

Received: May 11, 2021
Accepted: July 21, 2021
Published: July 28, 2021

layer and the ambient conditions during the curing process, *i.e.*, relative humidity and temperature.[22]

Moisture-cure adhesives are referred to as the one-component adhesives that react with water in the atmosphere.[23] In the market, we can find cyanoacrylates and isocyanates that react with catalytic amounts of water, producing polymers by addition or chain-growth polymerization, or with stoichiometric amounts of water, producing polymers by condensation or step-growth polymerization.[24]

The most widely used one-component isocyanate adhesive is PMDI (polymeric methylene diphenyl diisocyanate),[25,26] which is a dark brown, viscous-liquid, aromatic chemical that contains between 30 and 80% of the monomer MDI (methylene diphenyl diisocyanate) together with oligomers with a degree of polymerization from 3 to 5, resulting in mixtures of an averaged functionalization of 2.7 isocyanate groups per molecule.[27] It has been used for more than 40 years as a cold-setting structural adhesive for the production of glued-laminated timber (glulam), and it exhibits superior water resistance performance than formaldehyde-based adhesives.[28]

So far, there has been made no use of aliphatic isocyanates for the production of one-component isocyanate adhesives nor in the control of the molecular architecture of this kind of reagents in order to tune the mechanical and thermal properties of such adhesives. The advantages of using aliphatic isocyanates are related to their lower toxicity and reactivity compared to aromatic isocyanates,[27] better durability, resistance to hydrolysis and oxidation, and stability when exposed to light, which make them an ideal candidate for the development of high-performance engineered adhesives.

In this work, a series of new aliphatic tetraisocyanates is studied for their use as moisture-cure adhesives or sealants, leading toward the formation of 100% polyurea networks. Such cured one-component isocyanates are block copolymers with microphase-separated hard and soft domains that result in materials with two glass transitions, a chemical (covalent bonds) network and a physical (hydrogen bonds) network in a single product. By controlling the volume fraction, the chemical composition between the hard and soft domains is tuned, and viscoplastic and viscoelastic materials are produced with a wide range of mechanical, chemical, and thermal properties on-demand, with uses as adhesives or sealants.

EXPERIMENTAL SECTION

Materials. The four linear hydrophobic diamino-terminated polypropylene oxide Jeffamine D-230, J-D230, (M_n = 240 g/mol, ρ = 948 Kg/m^3, n = 2.5, PDI = 1.04), D-400, J-D400 (M_n = 460 g/mol, ρ = 972 kg/m^3, n = 6, PDI = 1.03), D-2000, J-D2000 (M_n = 2060 g/mol, ρ = 991 kg/m^3, n = 33, PDI = 1.02), D-4000, and J-D4000 (M_n = 4000 g/mol, ρ = 994 kg/m^3, n = 68, PDI = 1.02) were from Huntsman International LLC, and the triisocyanate Basonat HI-100, BHI, (M_n = 504 g/mol, ρ = 1174 kg/m^3) from BASF SE were used as received.

Synthesis of Aliphatic Polyisocyanates. The four aliphatic polyisocyanates (A-D230, A-D400, A-D2000, and A-D4000) are formed by the rapid chemical reaction between a triisocyanate and a diamine to build urea moieties with a ratio of 2:1 in acetone by dropping slowly the diamino-terminated polypropylene oxide solution to the triisocyanate BHI.

The typical procedure to obtain the reactive polymers with a solid content of 13% in weight is given from the synthesis of the tetraisocyanate A-D230. In two separate 30 mL flasks, the diamino-terminated polypropylene oxide J-D230 (0.5742 g in 10.00 g of acetone) and the triisocyanate BHI (2.4143 g in 10.00 g of acetone) were dissolved. The content of diamine was added dropwise to the triisocyanate solution and reacted for 30 min. The mixture was maintained for 1 h at room temperature, and the solvent evaporated under reduced pressure. The resulting viscous material was put in a glass capsule, and the casted film was allowed to react at 20 °C and 65% RH for 72 h to ensure a good cross-linking process, resulting in cured films of ca. 400 μm thickness.

Fourier Transform Infrared Spectroscopy. Fourier transform infrared (FT-IR) spectra were collected using a Nicolet iS50 FT-IR spectrometer, equipped with a diamond Pike GladiATR single attenuated total reflection (ATR) system. Samples were scanned over the range of 4000 to 600 cm^{-1}, with a resolution of 2 cm^{-1} and averaged over 64 scans.

Nuclear Magnetic Resonance Spectroscopy. Two-dimensional diffusion ordered spectroscopy (2D DOSY) ^{1}H NMR experiments were carried out on a Bruker Avance AVHD400 nuclear magnetic resonance (NMR) spectrometer operating at 400 MHz and using $CDCl_3$ as the solvent and as the internal standard. Samples were prepared with a final solid content concentration of 5% in weight.

Differential Scanning Calorimetry. Differential scanning calorimetry (DSC) experiments were carried out on a TA Q2000 DSC instrument, with an autosampler and with heating and cooling rates of 10 K/min under the nitrogen atmosphere, using 20 μL aluminum pans with holes. The first heating run was used to remove all effects because of the thermal history of the elastomer, and only second heating was used for the evaluation of the samples.

Small-Angle X-ray Scattering. Small-angle X-ray scattering (SAXS) experiments were performed using a Rigaku BioSAXS-1000 equipped with an HF007 microfocused beam (1.2 kW; 40 kV; 30 mA), with $\lambda_{CuK\alpha}$ = 0.15418 nm radiation collimated by specially designed two-mirror focusing optics and a Kratky block to obtain direct information on the scattering patterns. The SAXS intensity was collected using a 2D Rigaku HyPix-3000 X-ray detector (77.5 cm × 38.5 cm, 100 μm resolution). An effective scattering vector range of 0.08 /nm^{-1} < q < 6 nm^{-1} was obtained, where q is the scattering wave vector.

Wide-Angle X-ray Scattering. Wide-angle X-ray scattering (WAXS) experiments were performed using a Bruker D8 Advance Eco (goniometer radius of 250 mm; 2° < 2θ < 40°, $\Delta\theta$ = 0.01°, 19.2 s/step) equipped with a copper tube (1 kW; 40 kV; 25 mA), with $\lambda_{CuK\alpha}$ = 0.15418 nm radiation, collimated using an automatic divergent slit (15 mm) and a primary soller (2.5°) to obtain direct information on the scattering patterns. The WAXS intensity was collected after a secondary soller (2.5°) using a one-dimensional (1D) Lynxeye XE-T detector (3.296° opening). An effective scattering vector range of 2 nm^{-1} < q < 25 nm^{-1} was obtained, where q is the scattering wave vector.

Tension Stress–Strain. Tension stress–strain (TSS) measurements were performed with a self-constructed custom-built single-column tensile testing machine for polymer film testing at 20 °C and the strain rate of 1.66·10^{-4} s^{-1}. The samples were stretched using a parallel clamping system mounted to a ballscrew-actuated linear axis with a VEXTA SH-type microstep motor, controlled using a TB6600 microstep controller via a custom LabVIEW-based software. The force and deformation were measured using an HBM S2 transducer load cell (±100 N, accuracy class 0.02) and an HBM KW3073 high-performance strain gauge indicator, respectively. For the acquisition of measurement data, an HBM QuantumX MX410 was used.

Dynamic Mechanical Analysis. Dynamic mechanical analysis (DMA) temperature- and frequency-sweep experiments were performed to measure the temperature and frequency behaviors of the samples using a Diamond DMA and DMA 8000, respectively. The temperature sweeps were conducted at a heating temperature rate of 2 K/min in the temperature region from 160 to 375 K at frequencies of 0.1, 1, 10, and 70 Hz. The frequency sweeps were conducted at 20 °C in the range from 0.1 to 40 Hz. The samples were fixed in a special holder for the tension geometry, and all experiments were performed under N_2 atmosphere.

https://doi.org/10.1021/acsapm.1c00578
ACS Appl. Polym. Mater. 2021, 3, 4070−4078

Scheme 1. Chemical Structure of the Tetrafunctionalized Aliphatic Polyisocyanates (A-D230, A-D400, A-D2000, and A-D4000) with an Aliphatic Triisocyanate (red) at Both Extremes of the Soft Polypropylene Oxide Backbone (blue) with the Two Urea Motifs (Purple) Connecting Both the Soft and Hard Segments

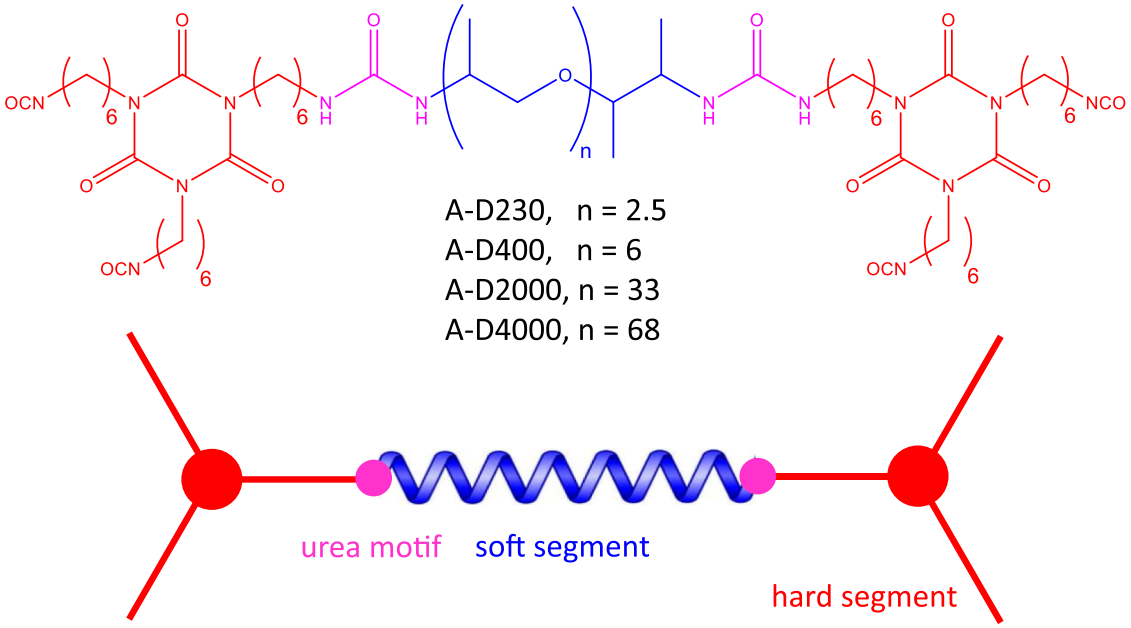

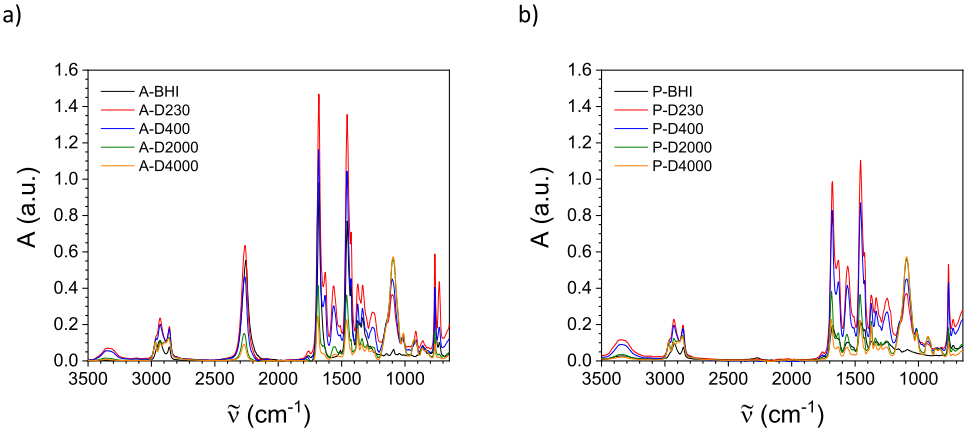

Figure 1. FT-IR spectra for (a) the four aliphatic polyisocyanates (A-D230, A-D400, A-D2000, and A-D4000) and (b) the corresponding polyurea networks (P-D230, P-D400, P-D2000, and P-D4000). Note: the reference reactive polymer (A-BHI) and the corresponding cured reference polyurea network (P-BHI) are also shown in black.

RESULTS AND DISCUSSION

Synthesis and Characterization of Aliphatic Polyisocyanates and Polyurea Networks. Four aliphatic polyisocyanates were synthesized by attaching an aliphatic triisocyanate molecule (A-BHI, the reference reactive polymer) at each extreme of a monodisperse soft polymer segment (J-D230, J-D400, J-D2000, and J-D4000) diamino-terminated polypropylene oxide in acetone and at room temperature, and forming the corresponding tetraisocyanate structure (A-D230, A-D400, A-D2000, and A-D4000) containing two urea motifs (Schemes 1 and S1). The resulting aliphatic polyisocyanates were cured at 20 °C and 65% relative humidity for 72 h. In this way, water molecules react with the isocyanate groups delivering free amines after the emission of a carbon dioxide molecule per reacted water molecule that react with the rest of isocyanates, forming new urea linkages. The resulting aliphatic polyurea networks or cured aliphatic polyisocyanates (P-D230, P-D400, P-D2000, and P-D4000) contain soft and hard segments (Scheme 1 and S1) that are microphase-segregated,[29] and they are very attractive materials because they do not require a catalyst and show enhanced chemical resistance and mechanical properties compared to the polyurethane counterparts.[30,31]

The enthalpies for the hydrolysis of an amide, carbamate, and urea linkage are *ca.* 75, 145, and 160 kJ/mol, respectively, based on the enthalpies of formation. In addition, we can also consider the extra energy factor from the removal of the hydrogen bonds (from 15 to 25 kJ/mol, depending on the distance and angle), which might be more than double (50 kJ/mol or higher) for polyurea systems because of the bidentate nature of the hydrogen bonding between urea motifs.

FT-IR experiments were performed to ensure the full curing of the reactive polymers. The aliphatic polyisocyanates were analyzed by FT-IR, showing the characteristic peaks from the isocyanate groups at 1334−1372 cm^{-1} (N═C═O ν_s) and

https://doi.org/10.1021/acsapm.1c00578
ACS Appl. Polym. Mater. 2021, 3, 4070−4078

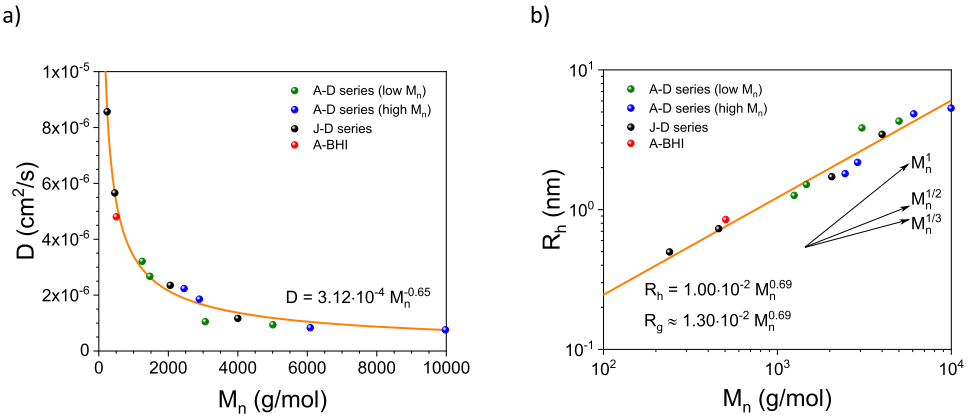

Figure 2. (a) Diffusion coefficient, D, (b) hydrodynamic radius, R_h, for the four aliphatic polyisocyanates (A-D230, A-D400, A-D2000, and A-D4000), diamino-terminated polypropylene oxide polymers (J-D230, J-D400, J-D2000, and J-D4000), and the reference reactive polymer (A-BHI) as a function of the molar mass, M_n.

Table 1. WAXS and SAXS Analyses Showing the Interchain Scattering Peak (q_{W1}), the Isocyanurate Scattering Peak (q_{W2}), and the Microphase Separation Scattering Peak (q_{S1}) with the Corresponding Distances (d_{W1}, d_{W2}, and d_{S1}) and Correlation Lengths (ξ_{W1}, ξ_{W2}, and ξ_{S1}) for the Four Aliphatic Polyurea Networks (P-D230, P-D400, P-D2000, and P-D4000) and the P-BHI

sample	q_{W1} (nm^{-1})	d_{W1} (nm)	ξ_{W1} (nm)	q_{W2} (nm^{-1})	d_{W2} (Å)	ξ_{W2} (Å)	q_{S1} (nm^{-1})	d_{S1} (nm)	ξ_{S1} (nm)
P-D230	14.4	4.4	13.4	7.83	0.80	2.00	2.93	2.14	1.29
P-D400	14.4	4.4	12.9	7.99	0.79	1.95	1.31	4.80	1.74
P-D2000	14.2	4.4	12.9	9.53	0.66	1.09	1.10	5.73	7.57
P-D4000	14.3	4.4	12.8	10.36	0.61	0.97	0.81	7.71	13.71
P-BHI	14.5	4.3	14.9	7.87	0.80	2.14	0.89	7.07	5.43

2262 cm^{-1} (N═C═O ν_{as}), the methylene groups at 764 cm^{-1} (CH_2 ρ) and 1457 cm^{-1} (CH_2 δ), the isocyanurate ring at 1680 cm^{-1} ($[NCO]_3$), the ether groups at 915 cm^{-1} (CH−O−CH_2 ν_s) and 1094 cm^{-1} (CH−O−CH_2 ν_{as}), and the urea groups at 1629 cm^{-1} (C═O amide I), 1563 cm^{-1} (CO−N−H amide II), and 3335 cm^{-1} (N−H ν, hydrogen-bonded), as shown in Figure 1a.[32,33] After curing the samples, the peak corresponding to the free isocyanate reactive group at 2262 cm^{-1} completely disappeared, with an increase in the intensity of the peaks corresponding to the formation of new urea groups (1629 and 1563 cm^{-1}) and hydrogen bonding (3335 cm^{-1}), as indicated in Figure 1b. The results show the complete reaction of the isocyanate groups after the curing process with the corresponding polyurea network formation (Figure S1).

DOSY ^{1}H NMR experiments were carried out for the evaluation of the diffusion coefficient and the radius of the polymer in solutions for each reactive polymer, as well as for the genitor diamino-terminated polypropylene oxide polymer (Figure S2). This technique allows for the correlation of the molar mass of these polymers, while other techniques, e.g., gel permeation chromatography (GPC) or matrix-assisted laser desorption ionization time-of-flight (MALDI-TOF), could not be used because of the high reactivity of isocyanate groups. Polyetheramines are single-component molecules, while all reactive polymers have two main components as, indicated in the left y-axis projection of intensities where two peaks are observed. The second high molar-mass component, the dimer, originates from the reaction of the low molar-mass component, the targeted reactive polymer (Schemes 1 and S1), which reacts with a residual water molecule in deuterated chloroform. Therefore, carbamic acid is produced, which releases carbon dioxide and delivers free amine. This *in situ*-generated amine will react with an isocyanate group, forming a urea bridge between two reactive polymers connecting two hard segments and generating a hexaisocyanate. By comparing each reactive polymer to its corresponding genitor polymer, a clear change in the diffusion coefficient is evidenced from the lower position of the NMR signals in the y-scale (Figure S2).

The diffusion coefficient was calculated by the regression analysis from the change in the normalized signal intensity, I_{norm}, of an NMR peak belonging to the molecule to be studied as a function of the square of the strength of the gradient pulse, G^2, by fitting the data to a modified Stejskal−Tanner function (Eq. S1 and Figure S3).[34,35] Figure 2a shows the diffusion coefficient, D, for the four aliphatic polyisocyanates, the four diamino-terminated polypropylene oxide polymers and the reference reactive polymer as a function of the molar mass, M_n.

The hydrodynamic radius, R_h, was calculated following the Stokes−Einstein equation (eq S2), with a scaling factor, f (eq S3 and Figure S4),[36] and the radius of gyration, R_g, assuming an average ratio of R_h/R_g = 0.769 in chloroform (Figure 2b).[37] The diffusion coefficient and both radii follow a power-law behavior, with an exponent of −0.65 and 0.69, respectively, consistent with previous results,[38] and they are summarized in Table S1 together with the Stokes−Einstein scaling factor, f. Therefore, this synthetic approach for obtaining well-defined aliphatic polyisocyanates gives a high level of control over the chemical structure of these reactive polymers. A calibration curve can be constructed for the molar mass determination when other techniques are not suitable because of the high reactivity of the polymers that react with the matrix or the solvent.

Thermal, Structural, and Mechanical Properties of the Aliphatic Polyurea Networks. WAXS and SAXS experiments were conducted in order to elucidate the

https://doi.org/10.1021/acsapm.1c00578
ACS Appl. Polym. Mater. 2021, 3, 4070−4078

amorphous nature of the cured polyisocyanates, as well as the microphase separation between the hard and the soft domains. WAXS analysis (Table 1 and Figure S5a) showed the amorphous nature (glassy or rubber-like) of all cured aliphatic polyisocyanates, as could be observed by the presence of a main broad peak at q_{W1} = 14.4 nm^{-1} that corresponds to an interchain distance between the polymers of both hard (polymethylene) and soft domains (polypropylene oxide) of d_{W1} = 4.4 Å. A secondary broad peak at q_{W2} = 8 to 10 nm^{-1} was also present corresponding to the distance between the isocyanurate rings within the hard domains of d_{W2} = 8 to 6 Å. The amorphous nature of all aliphatic polyurea networks was confirmed by the average correlation length of ξ_{W1} = 13 Å and ξ_{W2} = 1 to 2 nm related to 2 to 3 repeating units in both the hard and soft domains.

SAXS analysis (Table 1 and Figure S5b) clearly indicates the block copolymer nature with the microphase separation between the domains of these cured materials by the presence of a peak, q_{S1}, at 2.9, 1.3, 1.1, and 0.8 nm^{-1} for the polyurea networks P-D230, P-D400, P-D2000, and P-D4000, respectively, which is attributed to the average distance between the hard and soft domains.[29,39] The resulting microphase separation distance, d_{S1}, has values of 2.1, 4.8, 5.7, and 7.7 nm when increasing the polypropylene oxide molar mass (240, 460, 2056, and 4000 g/mol) connecting two triisocyanates molecules (Scheme 1). These results are in line with the increased volume fraction of the soft domains, ϕ_{PPO}, (0.23, 0.36, 0.71, and 0.82) and the contour length, l_c, from molecular mechanic simulations (MM2), resulting in 3.3, 4.3. 13.9, and 26.4 nm, which indicates the random packing of the polymer chains within the corresponding domains.

DSC experiments were conducted for the identification of the amorphous nature of these materials, together with the glass transition of both hard and soft domains and the presence of hydrogen bonding related to the presence of a transient network.[33] The presence of the disubstituted urea motifs allows for the formation of well-ordered hydrogen bonds that lead to the formation of a transient network, which vanishes upon heating the polyurea networks at temperatures above 60 to 90 °C.

The first heating run showed an endothermic peak corresponding to the removal of hydrogen bonds between the urea motifs connecting hard and soft domains. The values of the maximum of these peaks do not follow any tendency and range from 60 to 100 °C (Table 2 and Figure S6). Because of the fast cooling and heating rates (10 K/min), there was no presence of such hydrogen bonds in the second heating run. Therefore, lower temperature rates or longer times are needed for restoring all hydrogen bonds and regenerating this transient network.[33]

Table 2. Glass Transition Temperatures for the Soft ($T_{g,PPO}$) and Hard ($T_{g,X}$) Domains with the Corresponding Heat Capacities ($\Delta C_{p,PPO}$ and $\Delta C_{p,X}$) together with the Peak Maximum for the Removal of Hydrogen Bonds (T_{HB}) of the Four Aliphatic Polyurea Networks (P-D230, P-D400, P-D2000, and P-D4000) and the P-BHI

sample	$T_{g,PPO}$ (°C)	$\Delta C_{p,PPO}$ (J/mol K)	$T_{g,X}$ (°C)	$\Delta C_{p,X}$ (J/mol K)	T_{HB} (°C)
P-D230	43	0.244	-4	0.102	98
P-D400	33	0.339	−5	0.084	63
P-D2000	−58	0.417	−8	0.037	71
P-D4000	−66	0.482	−10	0.018	61
P-BHI			−7	0.139	65

All polyurea networks showed two glass transitions: one corresponding to the hard domains with an almost constant $T_{g,X}$-value from −4 to −10 °C and a second glass transition, $T_{g,PPO}$, attributed to the soft domains, which decreases from 45 to −65 °C upon increasing the molar mass of the polypropylene oxide polymer (Table 2 and Figure S6). Therefore, these networks are amorphous in nature being glasses or elastomers for the ones with a short (P-D230 and P-D400) or long (P-D2000 and P-D4000) polyether chain, respectively. Thus, the cured polyisocyanates are microphase-separated networks[40,41] determined by the presence of two glass transitions and heat capacity values, which match the theoretical values when taking into account the corresponding volume fractions. Therefore, the analysis from the heat capacities yields theoretical values for the hard and soft domains of $\Delta C_{p,PPO}$ = 0.137 J/mol/K and $\Delta C_{P,X}$ = 0.537 J/mol/K, respectively, when considering volume fraction values equal to one (Figure S7).

DMA temperature-sweep experiments were conducted on the four aliphatic polyurea networks (P-D230, P-D400, P-D2000, and P-D4000) and the P-BHI at the frequency values of 0.1, 1, 10, and 70 Hz (Figure 3 and Figure S8). For all the polyurea networks, two α-relaxation processes, glass transitions ($T_{g,PPO}$ and $T_{g,X}$), one β-relaxation process (T_β), and the melting of the hydrogen bonds (T_{HB}) from the urea motifs were detected (Figure 3a), and they are summarized in Tables S2, S3, and S4. While the glass transition of the hard domains ($T_{g,X}$) ranges from −35 to −5 °C at 1 Hz upon decreasing the volume fraction of the isocyanate component, the glass transition of the soft domains ($T_{g,PPO}$) was between 45 and 35 °C (P-D230 and P-D400) and between −50 and −60 °C (P-D2000 and P-D4000) for the short and long polypropylene oxide polymers, respectively, as shown in Figure 3a. The β-relaxation process (T_β) appears at very low temperatures, between −75 and −100 °C,[42,43] while the removal of hydrogen bonds (T_{HB}) occurs between 50 and 90 °C, approximately.[32−44]

All relaxation processes (α- and β-relaxation processes) showed a frequency dependence. Therefore, from the peak maximum in the loss factor profile, tan δ, or in the loss modulus profile, E'', at different frequencies, the activation energy, E_a, for every process was determined (Table 3 and Figure S9). The Arrhenius-like fitting of the data shows activation energy values between 50 and 60 kJ/mol/K for the segmental motions of all polymers, β-relaxation process; in addition, between 90 and 160 kJ/mol/K and between 250 and 475 kJ/mol/K for the glass transition, α-relaxation process, within the hard and soft domains, respectively.[45−47]

When plotting the activation energy as a function of the hard domain volume fraction, ϕ_X (Figure S10a), or the segmental molecular weight, M_c (Figure S10b), the activation energy of the β-relaxation process is almost constant. Therefore, all segmental motions are independent of the chemical composition of the reactive polymer, but a different behavior is observed for the two α-relaxation processes. There is a critical volume fraction $\phi_X^* \approx 0.47$ that corresponds to a critical segmental molecular weight of $M_c^* \approx 1000$ g/mol or a molar mass of the polypropylene oxide chain of $M_n^* \approx 750$ g/mol.

https://doi.org/10.1021/acsapm.1c00578
ACS Appl. Polym. Mater. 2021, 3, 4070−4078

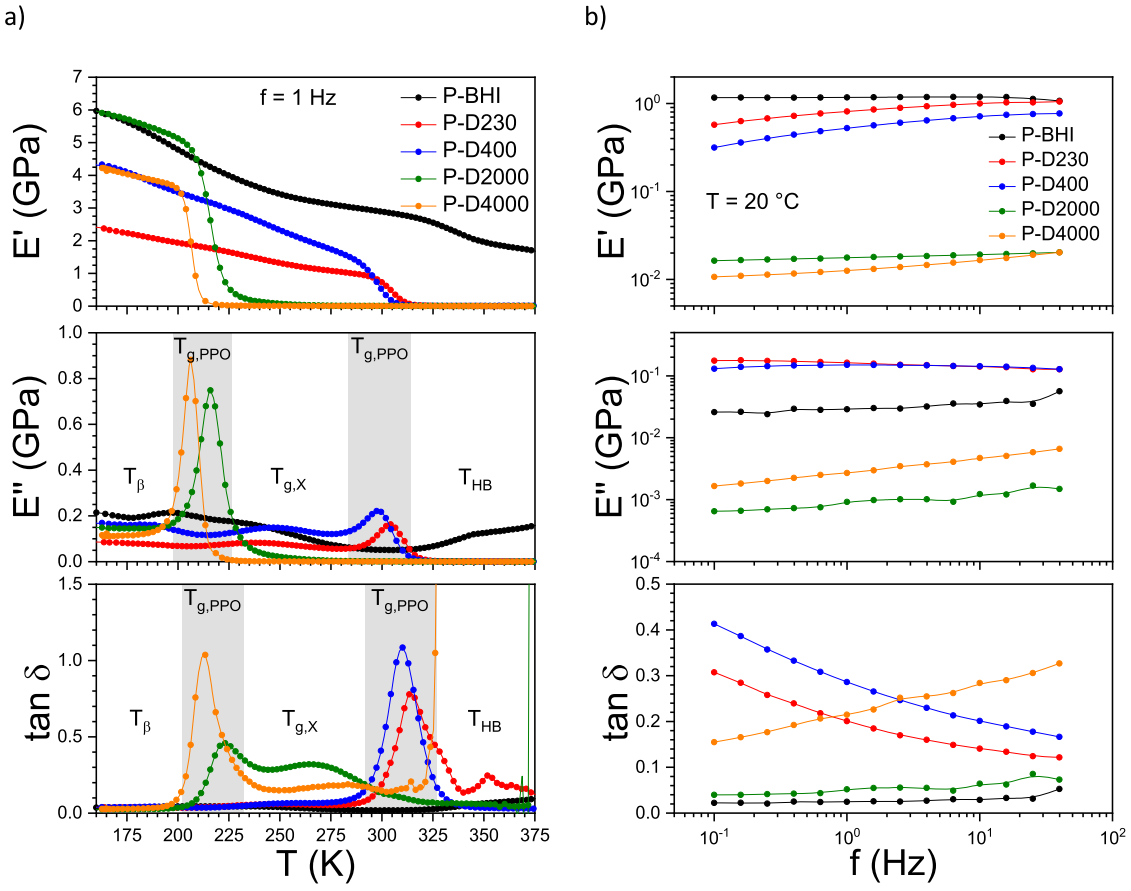

Figure 3. (a) DMA temperature-sweep experiments at f = 1 Hz and (b) DMA frequency-sweep experiments at T = 20 °C for the four aliphatic polyurea networks (P-D230, P-D400, P-D2000, and P-D4000) and the P-BHI. The gray areas correspond to the temperature range where the glass transition of the soft segments ($T_{g,PPO}$) was detected.

Table 3. Activation Energy of the Three Relaxation Processes ($E_{a,\beta}$, $E_{a,X}$, and $E_{a,PPO}$) for the Four Aliphatic Polyurea Networks (P-D230, P-D400, P-D2000, and P-D4000) and the P-BHI Determined from the Peak Maximum in the Loss Factor Profile, tan δ (Left), and in the Loss Modulus Profile, E" (Right), at Different Frequencies

	tan δ			E"		
sample	$E_{a,\beta}$ (kJ/mol)	$E_{a,X}$ (kJ/mol)	$E_{a,PPO}$ (kJ/mol)	$E_{a,\beta}$ (kJ/mol)	$E_{a,X}$ (kJ/mol)	$E_{a,PPO}$ (kJ/mol)
P-D230	56 ± 5	91 ± 7	476 ± 1	54 ± 5	82 ± 13	450 ± 1
P-D400	51 ± 2	140 ± 9	348 ± 1	52 ± 2	72 ± 5	375 ± 1
P-D2000	57 ± 10	157 ± 1	263 ± 1	71 ± 4	138 ± 4	252 ± 1
P-D4000	62 ± 13	n.d.	262 ± 1	n.d.	110 ± 7	258 ± 1
P-BHI	61 ± 1	89 ± 1		60 ± 2	102 ± 1	

Below this critical value, the two short polymers in P-D230 and P-D400 show a high activation energy value of 350-480 kJ/mol/K compared to the long polypropylene oxide chains in P-D2000 and P-D4000 with an activation energy of *ca.* 260 kJ/mol/K. This phenomenon could be explained because of the high volume fraction of hard domains in P-D230 and P-D400, which turns into a short distance between such hard domains, restricting the mobility of the soft polymers within the soft domains. Parallel to this observation, the polymethylene chains within the hard domains are also affected above this critical value. The short polypropylene oxide chains in the soft domains disturb the hard domains, leading to a lower activation energy of *ca.* 90 kJ/mol/K when compared to the long soft chains of *ca.* 160 kJ/mol/K.

DMA frequency-sweep experiments were also conducted on the four cured polyisocyanates at 20 °C from 0.1 to 40 Hz (Figure 4b). While for the short polymers, a glassy-like behavior is detected, and the long polymers are in the rubber-like region, as indicated by a master curve obtained using the time−temperature superposition method (Figure S11). For the short aliphatic polyurea networks (P-D230 and P-D400), the presence of the soft domains with reduced mobility greatly affects the viscoplastic behavior[48] of these materials when compared to the reference cured sample P-BHI showing lower elastic modulus values (69 and 45%) while increasing the loss modulus (6 to 7 times), respectively (Table S5). Thus, upon adding these soft segments, a damping component is introduced in the sample while sacrificing a portion of the elastic properties of the P-BHI and making the material less brittle. For the viscoelastic long polypropylene oxide-containing polyurea networks P-D2000 and P-D4000, the elastic and the loss modulus decreased to 1.5 and 1.1%, as well

https://doi.org/10.1021/acsapm.1c00578
ACS Appl. Polym. Mater. 2021, 3, 4070−4078

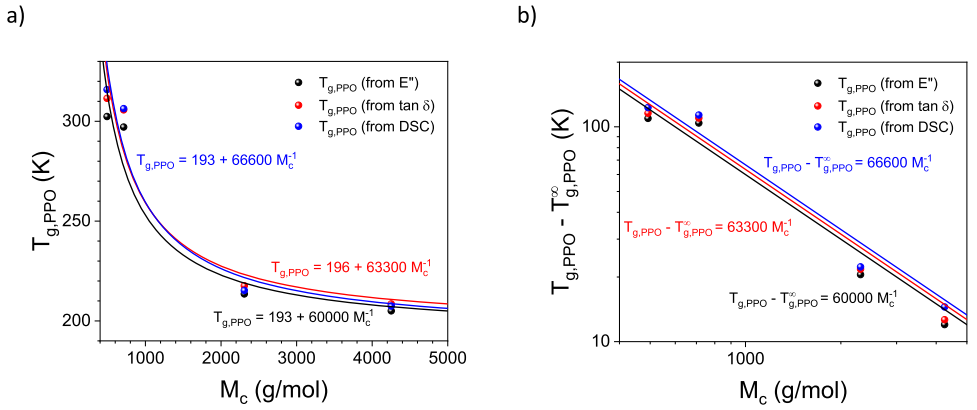

Figure 4. (a) Linear−linear plot and (b) log−log plot for the variation of the glass transition temperature, $T_{g,PPO}$, of the soft segment as a function of the segmental molecular weight, M_c, for the four aliphatic polyurea networks (P-D230, P-D400, P-D2000, and P-D4000). $T^{\infty}_{g,PPO}$ is the extrapolated glass transition temperature at infinitum segmental molecular weight from the Fox−Flory empirical model.

Table 4. Storage Modulus (E') from DMA Temperature- and Frequency-Sweep Experiments at 20 °C and 0.1 Hz, from TSS Experiments at 20 °C and $1.66 \cdot 10^{-4}$ s^{-1} Strain Rate, and from DMA Temperature-Sweep Experiments at 80 °C and at 0.1 Hz for the Four Aliphatic Polyurea Networks (P-D230, P-D400, P-D2000, and P-D4000) and the P-BHI, Together with the Corresponding Segmental Molecular Weight, M_c

		DMA T-sweep	DMA f-sweep	TSS	DMA T-sweep
sample	M_c (g/mol)	E'_{293} (GPa)	E'_{293} (GPa)	E'_{293} (GPa)	E'_{353} (GPa)
P-D230	492	0.579	0.574	0.112	0.00995
P-D400	712	0.360	0.316	0.0890	0.00900
P-D2000	2308	0.00650	0.0163	0.0148	0.00372
P-D4000	4252	0.00210	0.0107	0.00827	0.00137
P-BHI	226	2.860	1.166	0.846	1.703

as 3.2 and 9.3%, respectively, when compared to the P-BHI sample. In any case, the presence of these soft domains resulted in loss factors 10 times higher than the pure, cured isocyanate system P-BHI.

Comparing the results from the DSC, DMA, and TSS experiments allows for the evaluation of the effect that the segmental molecular weight and degree of polymerization has on the network's glass transition temperature and the mechanical properties. More precisely, decreasing the polymer length between the cross-linking points increases the glass transition temperature, $T_{g,PPO}$ (Figure 4), as observed when the Fox−Flory empirical model is applied (eq S4).[49−51] Therefore, the results show that the short polymers increase the glass transition temperature because of the low mobility of the polymer segments between the cross-linking points.

When comparing the storage modulus from different experiments at 20 °C, i.e., DMA temperature- and frequency-sweep experiments and TSS experiments (Figure S12), in the glassy state (P-D230 and P-D400) or in the transient network (P-D2000 and P-D4000), comparable results were obtained (Table 4). Even though no direct connection can be made because of the different nature of the samples at this temperature, glass or rubber, a power law tendency could be observed, as shown in Figure 5. When analyzing the storage modulus in the rubbery plateau at 80 °C, after the removal of the hydrogen bonds between the urea motifs, a power law with an exponent of −1 was obtained with an average density of ρ = 0.75 g/mol at 80 °C when considering a Poisson's ratio of ν = 0.5. This value is in line with the density of all diamino-terminated polypropylene oxide polymers (from 0.95 to 0.99 g/mol at 25 °C) and the aliphatic polyurea networks (from 1.03 to 1.12 g/mol at 25 °C), showing good agreement

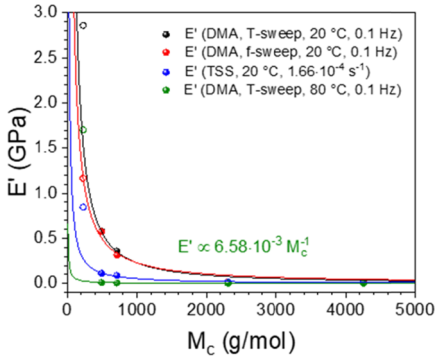

Figure 5. Storage modulus, E', as a function of the segmental molecular weight, M_c, for the four aliphatic polyurea networks (P-D230, P-D400, P-D2000, and P-D4000) and the P-BHI evaluated from the DMA temperature-sweep experiments (black: at 20 °C and 0.1 Hz), the DMA frequency-sweep experiments (red: at 20 °C and 0.1 Hz), and the TSS experiments (blue: at 20 °C and $1.66 \cdot 10^{-4}$ s^{-1}) in the transient network and from the DMA temperature-sweep experiments (green: at 80 °C and 0.1 Hz) in the rubbery plateau. Note: the black, red, and blue lines are the guide to the eye, while the green line is the fit to the data in the rubbery plateau.

between the mechanical experiments and the chemistry of these reactive polymers.

CONCLUSIONS

A series of new aliphatic polyisocyanates has been synthesized by reacting diamino-terminated polypropylene oxide polymers to a trifunctionalized aliphatic isocyanate with the formation of a highly stable urea motif connecting both components. The

https://doi.org/10.1021/acsapm.1c00578
ACS Appl. Polym. Mater. 2021, 3, 4070−4078

resulting reactive polymers have a well-defined structure with a monodisperse and higher degree of functionalization (n = 4) and are less toxic than the commercially available aromatic polydisperse polyisocyanates, e.g., PMDI, which normally are of lower functionality (*ca.* n = 2.7). Having control on the chemistry and functionalization, as well as on the chemical structure of the reactive polymer, allows for obtaining clear-cut polyurea networks when the polyisocyanates are cured at 20 °C and 65% RH, the water molecules being responsible for the curing process.

The resulting aliphatic polyurea networks are amorphous block copolymers in nature as shown by DMA, WAXS, SAXS, and DSC experiments, and because of the microphase separation of both the hard and soft domains, two glass transition temperatures are present. The glass transition temperature of the soft domains, which can be allocated above (at room temperature) or below (at subzero temperature) the glass transition temperature of the hard domains for the short and long polymer chains, respectively, is strongly affected by the degree of polymerization of the polypropylene oxide polymer. This results in materials with viscoplastic or viscoelastic properties by tuning the length of the soft polymer segment.

Moreover, these cured polyisocyanates show the presence of a transient network because of the formation of hydrogen bonds between the urea motifs when the isocyanate groups react first with moisture and afterward with the *in situ*-generated amines. Therefore, these materials show higher mechanical, thermal, and chemical performance than their polyurethane and polyamide counterparts.

Controlling the functionalization and the degree of polymerization of the soft segment results in obtaining reactive polymers that after moisture-curing have on-demand properties such as elastic modulus, viscoplastic or viscoelastic properties, high softening temperatures, and chemical resistance. In this way, new polyisocyanates can be produced with a wide range of high-performance applications in the wood and construction industry, as well as for electronics, textiles, and medical devices.

Author Contribution. A. S. F. designed and performed the synthesis of the aliphatic polyisocyanates, FT-IR and NMR spectroscopy experiments, DSC thermal analysis experiments, evaluated and analyzed the DMA, TSS, SAXS and WAXS results, and wrote the manuscript. V. S. and W. S. performed the DMA experiments. M. E. constructed the small-scale TSS machine and performed the TSS experiments. R. S. performed the SAXS experiments. H. A. G. performed the WAXS experiments. V. S., M. E., R. S., H. A. G., and W. S. revised the manuscript. K. R. supervised the study and revised the manuscript.

■ ASSOCIATED CONTENT

Supporting Information

The Supporting Information is available free of charge at https://pubs.acs.org/doi/10.1021/acsapm.1c00578.

Additional characterizations; synthesis and reactivity of aliphatic tetraisocyanates; FT-IR spectra; 2D DOSY ^{1}H NMR spectra; diffusion coefficient calculation; Stokes−Einstein scaling factor; WAXS and SAXS intensity profiles; DSC thermograms; heat capacity evaluation; DMA temperature-sweep experiments; activation energy calculation; activation energy as a function of ϕ_X and M_c; DMA frequency-sweep experiments; TSS experiments; 2D DOSY ^{1}H NMR data; DMA temperature-sweep (tan δ) relaxation processes data; DMA temperature-sweep (E)" relaxation processes data; DMA temperature-sweep (tan δ) hydrogen-bonding data; DMA frequency-sweep data; and equations (PDF)

■ AUTHOR INFORMATION

Corresponding Authors

Antoni Sánchez-Ferrer − *School of Life Sciences, Wood Research Munich (HFM), Technical University of Munich, D-80797 Munich, Germany;* orcid.org/0000-0002-1041-0324; Email: sanchez@hfm.tum.de

Klaus Richter − *School of Life Sciences, Wood Research Munich (HFM), Technical University of Munich, D-80797 Munich, Germany*; Email: richter@hfm.tum.de

Authors

Viktor Soprunyuk − *Faculty of Physics, University of Vienna, A-1090 Vienna, Austria*

Max Engelhardt − *School of Life Sciences, Wood Research Munich (HFM), Technical University of Munich, D-80797 Munich, Germany*

Ralf Stehle − *Department of Chemistry, Technical University of Munich, D-85747 Garching, Germany*

H. Albert Gilg − *Department of Civil Geo and Environmental Engineering, Technical University of Munich, D-80333 Munich, Germany*

Wilfried Schranz − *Faculty of Physics, University of Vienna, A-1090 Vienna, Austria*

Complete contact information is available at: https://pubs.acs.org/10.1021/acsapm.1c00578

Notes

The authors declare no competing financial interest.

■ ACKNOWLEDGMENTS

The authors would like to thank Dr. Karin Kleigrewe from the Bavarian Center for Biomolecular Mass Spectrometry (BayBioMS - TUM) and Sandra Wenisch and Dr. Eliza Gemel from the Catalysis Research Center (CRC - TUM) for allowing us to measure MALDI-TOF and DSC, respectively.

■ REFERENCES

(1) Pethrick, R. A. Design and Ageing of Adhesives for Structural Adhesive Bonding. *Proc. Inst. Mech. Eng. Pt. L J. Mater. Des Appl. Ther.* **2015**, *229*, 349−379.

(2) Budhe, S.; Banea, M. D.; de Barros, S. Bonded Repair of Composite Structures in Aerospace Application. *Appl. Adhes. Sci.* **2018**, *6*, 1−27.

(3) Cavezza, F.; Boehm, M.; Terryn, H.; Hauffman, T. A Review on Adhesively Bonded Aluminium Joints in the Automotive Industry. *Metals* **2020**, *10*, 730−762.

(4) Emblem, A.; Hardwidge, M. *Adhesives for Packaging, in Packaging Technology: Fundamentals, Materials and Processes*; Woodhead Publishing, 2012.

(5) Bridarolli, A.; Odlyha, M.; Nechyporchuk, O.; Holmberg, K.; Ruiz-Recasens, C.; Bordes, R.; Bozec, L. Evaluation of the Adhesion and Performance of Natural Consolidants for Cotton Canvas Conservation. *ACS Appl. Mater. Interfaces* **2018**, *10*, 33652−33661.

(6) Aradhana, R.; Mohanty, S.; Nayak, S. K. A Review on Epoxy-Based Electrically Conductive Adhesives. *Int. J. Adhes. Adhes.* **2020**, *99*, 102596−102614.

(7) Yim, M. J.; Li, Y.; Moon, K.; Paik, K. W.; Wong, C. P. Review of Recent Advances in Electrically Conductive Adhesive Materials and Technologies in Electronic Packaging. *J. Adhes. Sci. Technol.* **2008**, *22*, 1593−1630.
(8) Sarvar, F.; Hutt, D. A.; Whalley, D. C. Application of Adhesives in MEMS and MOEMS Assembly. *2nd International IEEE Conference on Polymers and Adhesives in Microelectronics and Photonics. POLYTRONIC 2002*. Conference Proceedings (Cat. No.02EX599): Zalaegerszeg, Hungary, 2002, 22−28.
(9) Paiva, R. M.; Marques, E. A.; da Silva, L. F.; António, C. A.; Arán-Ais, F. Adhesives in the Footwear Industry. *Proc. Inst. Mech. Eng. Pt. L J. Mater. Des. Appl.* **2016**, *230*, 357−374.
(10) E., Stammen, K., Dilger, *Adhesive bonding of textiles: Principles and Applications, in Joining Textiles*; Ed. Jones, I.; Stylios, G.K., Woodhead Publishing, 2013, 275-308.
(11) Tout, R. A review of Adhesives for Furniture. *Int. J. Adhes. Adhes.* **2000**, *20*, 269−272.
(12) Thoma, C.; Konnerth, J.; Sailer-Kronlachner, W.; Rosenau, T.; Potthast, A.; Solt, P.; van Herwijnen, H. W. G. Hydroxymethylfurfural and its Derivatives: Potential Key Reactants in Adhesives. *ChemSusChem* **2020**, *13*, 5408−5422.
(13) Milia, E.; Cumbo, E.; Cardoso, R. J. A.; Gallina, G. Current Dental Adhesives Systems: A Narrative Review. *Curr. Pharm. Des.* **2012**, *18*, 5542−5552.
(14) Bouten, P. J. M.; Zonjee, M.; Bender, J.; Yauw, S. T. K.; van Goor, H.; van Hest, J. C. M.; Hoogenboom, R. The Chemistry of Tissue Adhesive Materials. *Prog. Polym. Sci.* **2014**, *39*, 1375−1405.
(15) Dinte, E.; Sylvester, B. *Adhesives: Applications and Recent Advances, in Applied Adhesive Bonding in Science and Technology*; IntechOpen, 2018.
(16) Rudawska, A. *Adhesives: Applications and Properties*; IntechOpen, 2016, DOI: 10.5772/62603.
(17) Kim, W. S.; Yun, I. H.; Lee, J. J.; Jung, H. T. Evaluation of Mechanical Interlock Effect on Adhesion Strength of Polymer−Metal Interfaces Using Micro-Patterned Surface Topography. *Int. J. Adhes. Adhes.* **2010**, *30*, 408−417.
(18) Frihart, C. R.; Hunt, C. G. *Adhesives with Wood Materials, in Wood Handbook: Wood as an Engineering Material*; Forest Products Laboratory, 2010.
(19) Pocius, A. V. *The Chemistry and Physical Properties of Structural Adhesives, in Adhesion and Adhesives Technology*; Carl Hanser Verlag, 2012.
(20) Burchardt, B. R.; Merz, P. W. Elastic Bonding and Sealing in Industry. *In Handbook of Adhesives and Sealants*; Elsevier, 2006. *2*.
(21) Segura, D. M.; Nurse, A. D.; McCourt, A.; Phelps, R.; Segura, A. Chemistry of Polyurethane Adhesives and Sealants. In *Handbook of Adhesives and Sealants*, Elsevier, 2005, *1*.
(22) Petrie, E. M. *Handbook of Adhesives and Sealants*; McGraw-Hill, 2000.
(23) Hartshorn, S. R. *Structural Adhesives*; Plenum Press, 1986.
(24) Chaudhury, M.; Pocius, A. V. *Adhesion Science and Engineering*; Elsevier, 2002, *2*.
(25) Richter, K.; Pizzi, A.; Despres, A. Thermal Stability of Structural One-Component Polyurethane Adhesives for Wood—Structure-Property Relationship. *J. Appl. Polym. Sci.* **2006**, *102*, 5698−5707.
(26) Vick, C. B.; Okkonen, E. A. Durability of One-Part Polyurethane Bonds to Wood Improved by HMR Coupling Agent. *Forest Prod. J.* **2000**, *50*, 69−75.
(27) DFG, Deutsche Forschungsgemeinschaft. *4,4̀-Methylene diphenyl isocyanate MDI and polymeric MDI PMDI, in Documentations and Methods, in The MAK-Collection Part I, MAK Value Documentations*; WILEY-VCH, 2015.
(28) Pizzi, A. *Wood Adhesives − Isocyanates/Urethanes, in Handbook of Adhesion*; John Wiley & Sons, 2005.
(29) Sebastián, N.; Contal, C.; Sánchez-Ferrer, A.; Pieruccini, M. Interplay Between Structure and Relaxation in Polyurea Networks: The Point of View from A Novel Method of Cooperativity Analysis of Dielectric Response. *Soft Matter* **2018**, *14*, 7839−7849.
(30) Berger, D. M.; Primeaux, II, D. J. *Thick-Film Elastomeric Polyurethanes and Polyureas, in The Inspection of Coatings and Linings*; The Society for Protective Coatings, 2003.
(31) Vilar, W. D. *Chemistry and Technology of Polyurethanes*; Vilar Polyurethanes, 2002.
(32) Sánchez-Ferrer, A.; Rogez, D.; Martinoty, P. Synthesis and Characterization of New Polyurea Elastomers by Sol-Gel Chemistry. *Macromol. Chem. Phys.* **2010**, *211*, 1712−1721.
(33) Sánchez-Ferrer, A.; Rogez, D.; Martinoty, P. Influence of the Degree of Polymerisation and of the Architecture on the Elastic Properties of New Polyurea Elastomers. *RSC Adv.* **2015**, *5*, 6758−6770.
(34) Cohen, Y.; Avram, L.; Frish, L. Diffusion NMR Spectroscopy in Supramolecular and Combinatorial Chemistry: An Old Parameter-New Insights. *Angew. Chem. Int. Ed.* **2005**, *44*, 520−554.
(35) Claridge, T. D. W. *Diffusion NMR Spectroscopy, in High-Resolution NMR Techniques in Organic Chemistry*; Elsevier, 2016.
(36) Chen, H. C.; Chen, S. H. Diffusion of Crown Ethers in Alcohols. *J. Phys. Chem.* **1984**, *88*, 5118−5121.
(37) Kok, C. M.; Rudin, A. Relationship between the Hydrodynamic Radius and the Radius of Gyration of a Polymer in Solution. *Makromol. Chem., Rapid Commun.* **1981**, *2*, 655−659.
(38) Fetters, L. J.; Hadjichristidis, N.; Lindner, J. S.; Mays, J. W. Molecular Weight Dependence of Hydrodynamic and Thermodynamic Properties for Well-Defined Linear Polymers in Solution. *J. Phys. Chem. Ref. Data Monogr.* **1994**, *23*, 619−640.
(39) Reinecker, M.; Soprunyuk, V.; Fally, M.; Sánchez-Ferrer, A.; Schranz, W. Two Glass Transition Behaviour of Polyurea Networks: Effect of the Segmental Molecular Weight. *Soft Matter* **2014**, *10*, 5729−5738.
(40) Sánchez-Ferrer, A.; Reufer, M.; Mezzenga, R.; Schurtenberger, P.; Dietsch, H. Inorganic-Organic Elastomer Nanocomposites from Integrated Ellipsoidal Silica-Coated Hematite Nanoparticles as Crosslinking Agents. *Nanotechnology* **2010**, *21*, No. 185603.
(41) Sánchez-Ferrer, A.; Mezzenga, R.; Dietsch, H. Orientational Behavior of Ellipsoidal Silica-Coated Hematite Nanoparticles Integrated within an Elastomeric Matrix and its Mechanical Reinforcement. *Macromol. Chem. Phys.* **2011**, *212*, 627−634.
(42) Kopal, I.; Harničárová, M.; Valíček, J.; Kušnerová, M. Modeling the Temperature Dependence of Dynamic Mechanical Properties and Visco-Elastic Behavior of Thermoplastic Polyurethane Using Artificial Neural Network. *Polymer* **2017**, *9*, 519−536.
(43) Dupenne, D.; Roggero, A.; Dantras, E.; Lonjon, A.; Pierré, T.; Lacabanne, C. Dynamic Molecular Mobility of Polyurethane by a Broad Range Dielectric and Mechanical Analysis. *J. Non Cryst. Solids* **2017**, *468*, 46−51.
(44) Mihut, A. M.; Sánchez-Ferrer, A.; Crassous, J. J.; Hirschi, L. A.; Mezzenga, R.; Dietsch, H. Enhanced Properties of Polyurea Elastomeric Nanocomposites with Anisotropic Functionalized Nanofillers. *Polymer* **2013**, *54*, 4194−4203.
(45) Menard, K. P.; Menard, N. *Time and Temperature Scans Part I and II, in Dynamic Mechanical Analysis*; Taylor and Francis, 2020.
(46) Groenewoud, W. M. *Characterisation of Polymers by Thermal Analysis*; Elsevier, 2001.
(47) Sepe, M. P. *Dynamic Mechanical Analysis for Plastics Engineering*; William Andrew Publishing, 1998.
(48) Rull, N.; Sánchez-Ferrer, A.; Frontini, P. M. Deformation Behavior of Crosslinked Polyurea Elastomers Obtained via Sol-Gel Chemistry: Experimental Determination and Constitutive Modelling. *EXPRESS Polym. Lett.* **2020**, *14*, 663−672.
(49) Fox, T. G.; Flory, P. J. Second-Order Transition Temperatures and Related Properties of Polystyrene I: Influence of Molecular Weight. *J. Appl. Phys.* **1950**, *21*, 581−591.
(50) Fox, T. G.; Flory, P. J. The glass temperature and related properties of polystyrene. Influence of molecular weight. *J. Polym. Sci.* **1954**, *14*, 315−319.
(51) Fox, T. G.; Loshaek, S. Influence of Molecular Weight and Degree of Crosslinking on The Specific Volume and Glass Temperature of Polymers. *J. Polym. Sci. A* **1955**, *15*, 371−390.